Drying of Glassy Polymer Varnishes: A Quartz Resonator Study

CHARLES BOUCHARD,[1,2] BEATRICE GUERRIER,[1] CATHERINE ALLAIN,[1] ALEXANDER LASCHITSCH,[1,2] ANNE-CLAIRE SABY,[1,2] DIETHELM JOHANNSMANN[2]

[1] Laboratoire Fluides, Automatique & Systèmes Thermiques, Bâtiment 502, Campus Universitaire, 91405 Orsay Cedex, France

[2] Max Planck Institut für Polymerforschung, Postfach 3148, 55021 Mainz, Germany

Received 26 September 1997; accepted 30 January 1998

ABSTRACT: We report on desorption measurements on polymeric thin films coated onto quartz crystal resonators. Due to the high sensitivity of quartz crystal microbalances, the experiments can be performed on very thin films, which have small diffusion time constants even in the glassy state. When drying is performed slowly enough, diffusion equilibrium can be maintained through the whole process of desorption, including the glassy domain. From these quasi-stationary pressure ramps, we derived the solvent chemical potential as a function of polymer volume fraction $\mu(\phi)$. The results fit well to a model recently proposed by Leibler and Sekimoto.[1] In addition, we have derived the mutual diffusion coefficient $D(\phi)$ from pressure step experiments. We observe a strong decrease of $D(\phi)$ for high polymer concentrations typical of hypodiffusive systems like polymers. We investigated the drying of an industrial varnish that is a blend of 2 copolymers as well as the drying of its components separately. Both the solvent chemical potential $\mu(\phi)$ and the mutual diffusion coefficient $D(\phi)$ of the blend interpolate between the respective quantities of the components. © 1998 John Wiley & Sons, Inc. J Appl Polym Sci 69: 2235–2246, 1998

Key words: glass transition; desorption; diffusion; blend; quartz crystal microbalance

INTRODUCTION

The drying of complex fluids such as polymer solutions or polymer dispersions is a topic of high interest both for technological application and for fundamental science.[2] As the requirements on coatings in terms of residual solvent content, mechanical toughness, tribological behavior, and optical appearance become more and more stringent, coating and drying are recognized as important processing steps. They demand careful engineering and detailed understanding. Of specific interest in the context of drying is the residual solvent content, which should be as low as possible for environmental reasons. This issue is of special importance in the food packaging industry. Apart from the final properties of the coating, the speed of drying frequently is of great concern in practice for the performance of the whole process.

Realistic modeling of the drying process encounters 3 principal difficulties, which are the possibility of lateral structure formation on a microscopic scale,[3] the strong dependence of solvent diffusivity on solvent content (hypodiffusive behavior) and the plasticizing effect of the solvent, and memory effects inside the polymer matrix when it enters the glass state.

Lateral structure formation is of minor concern for thin films. We neglect it in this context and

Correspondence to: C. Allain (allain@fast.fast.u-psud.fr).

Journal of Applied Polymer Science, Vol. 69, 2235–2246 (1998)
 CCC 0021-8995/98/112235-12

treat the system as one-dimensional. Hypodiffusive behavior, on the other hand, usually cannot be avoided. When the polymer concentration increases, the chain mobility decreases and solvent diffusion through the polymer matrix slows down.[4,5] This effect is most prominent when the film enters the glassy regime: the chains are frozen in. It results in characteristic drying kinetics in which the drying speed is limited by heat transfer and solvent evaporation into the gas phase only during the initial stage and by diffusion and chain relaxation at longer times.[6–8] If the solvent transport within the film is solely governed by diffusion (hypodiffusive diffusion or with constant diffusivity), the kinetics is called Fickian.

Hypodiffusive systems develop strong gradients of solvent concentration during swelling and drying. Also, if the solvent content at a given position changes rapidly with time, a system near glass transition may exhibit memory, and local mechanical equilibrium may no longer be achieved. In the glass state, the process of matrix contraction is slower than the experimental time scale. The solvent acts as a plasticizer modifying both the transport coefficients of the polymer matrix and the speed of mechanical relaxation. The interplay between solvent transport and mechanical relaxation has been investigated for the swelling of polymers. Various anomalous regimes such as pseudo-Fickian, Case II, 2-step, and sigmoidal have been identified and theoretically described.[2,9–12]

A quantity frequently used to assess the relative importance of diffusion and mechanical relaxation is the Deborah number,[13] as follows:

$$(\mathrm{DEB})_D = \frac{\tau_M}{\tau_D} \tag{1}$$

where τ_M is the mechanical relaxation time, and τ_D is the characteristic time of diffusion given by

$$\tau_D = \frac{L^2}{D} \tag{2}$$

with L the sample thickness, and D the mutual diffusion coefficient. For very high Deborah numbers (that is, in thin films or slow mechanical relaxation), the long-time sorption dynamics are governed by mechanical relaxation; whereas for low Deborah numbers (that is, in thick films or sufficiently fast mechanical relaxation), diffusion dominates.

The Deborah number depends on the sample thickness through diffusion time. The high sensitivity of quartz crystal microbalances opens the way to investigations in a large range of Deborah numbers.[14] For polymer films in submicron range, the diffusion time at the glass transition is in the range of some seconds to some minutes. It is then possible to perform quasi-stationary drying experiments in which the experimental time scale is long compared to the diffusion time scale. In this case, diffusion equilibrium is approximately maintained throughout the experiment; the solvent concentration is always almost homogeneous. Note that while diffusion equilibrium is closely approached, mechanical equilibrium is not.

The process of drying has been investigated much less than sorption (that is, swelling).[15] Clearly, the phenomenology is different because during drying the material layer next to the vapor–film interface is the driest part of the sample and can act as a barrier blocking further solvent transport to the film surface. Such a dry skin can substantially slow down the drying, a phenomenon that is to be avoided in industrial process. Viscoelastic memory may further complicate the situation.

Although *in situ* structural investigations, as they have been carried out for swelling with forward recoil spectrometry[16] or Rutherford backscattering,[17,18] are certainly desirable for the drying of complex fluids, such investigations are probably too complicated to be performed on a wide variety of industrial systems, in which a large range of experimental parameters has to be covered. Careful integral measurements of solvent mass versus solvent vapor pressure are therefore an important task. These measurements are much easier and can still give valuable insight. This work deals with the estimation of solvent chemical potential $\mu(\phi)$ and solvent diffusivity $D(\phi)$ as a function of polymer volume fraction ϕ. The focus is on large polymer concentrations in the vicinity of glass transition. The functions $\mu(\phi)$ and $D(\phi)$ are an input to any model of the drying process, including much more complicated processes like fast swelling or fast drying by large amounts of solvent.[6,7,19]

We investigated 3 materials, as follows: an industrial varnish, which is a blend of 2 copolymers, and both the constituent copolymers separately. The films were spin-coated onto a quartz crystal, which was mounted in a vacuum chamber. When solvent vapor is admitted to the chamber, the film swells. The follows 2 types of experiments were performed: (a) quasi-stationary desorption (slow,

decreasing pressure ramps) and (b) pressure steps. From the quasi-stationary desorption, we obtained the solvent chemical potential $\mu(\phi)$. From the short-time kinetics following pressure steps, the mutual diffusion coefficient $D(\phi)$ was derived.

THEORETICAL BACKGROUND

Solvent Chemical Potential

The solvent chemical potential $\mu(\phi)$ can be derived from quasi-stationary sorption curves. Above the glass transition temperature of the solution, T_g, mechanical relaxation is fast, and the equilibrium sorption behavior can be described by the Flory–Huggins law[20]:

$$\mu(\phi, T) = kT[\ln(1 - \phi) + \phi + \chi\phi^2] \quad (3)$$

where k is the Boltzmann constant, T is the temperature, and χ is the polymer–solvent interaction parameter. The Flory–Huggins law predicts a smooth dependence of the solvent volume fraction $(1 - \phi)$ on vapor pressure P ($P = P_{sat}e^{\mu/kT}$, where P_{sat} is the saturation vapor pressure of pure solvent) with a positive curvature everywhere.

If the experiment is performed below the glass transition temperature T_g, the Flory–Huggins law is no longer adequate. One finds an excess solvent uptake at low vapor pressures, which is related to the fact that the polymer matrix can no longer contract on the envolved time scale. The curvature of the sorption curve is negative at low vapor pressures. This behavior is sometimes called Langmuir sorption.[21] The sorption–desorption curve has a clear kink at the point where the solvent-induced plastification is just sufficient to lower the glass transition temperature to the ambient temperature ($T_g(\phi) = T_{ambient}$).[22,23] We associate this kink with the (deswelling induced) glass transition. As always in the physics of glass-forming materials, the solvent volume fraction at the glass point $(1 - \phi_g)$ is not a variable of state; that is, ϕ_g depends on the sample history. For example, swelling of an annealed glassy film is expected to yield a value for ϕ_g different from the ϕ_g value obtained while drying the same film from the swollen state.

Leibler and Sekimoto[1] have revisited eq. (3) to take the elastic contribution of the glassy polymer matrix into account. They find

$$\mu(\phi, T) = kT[\ln(1 - \phi) + \phi + \chi\phi^2] - \nu_S K_{gl}^0 \ln\left(\frac{\phi}{\phi_g(T)}\right) \quad (4)$$

where ν_S is the solvent molecular volume. They assume that the polymer–solvent system is incompressible, and all loss of solvent is followed by matrix contraction. This contraction is ruled by the bulk osmotic modulus, $K = \phi(\partial\pi/\partial\phi)$, with π the osmotic pressure. Above the glass transition, no elastic contribution is envolved in K, and we get the Flory–Huggins relation [eq. (3)]. When the temperature decreases under the glass transition temperature, the polymer matrix contraction is opposed by an elastic contribution, which leads to an additional term in K, as follows: K_{gl}^0. Leibler and Sekimoto[1] assumes K_{gl}^0 to be constant and equal to the dry polymer osmotic modulus. While the osmotic modulus is entirely of entropic and enthalpic origin above the glass transition, an elastic contribution enters below.

Equation (4) qualitatively reproduces the excess solvent uptake in the glassy state. Mechanical relaxation could be incorporated into eq. (4) by making K_{gl}^0 dependent on time, which then, of course, removes the simplicity of the approach.

Mutual Diffusion Coefficient

Contrary to the case of $\mu(\phi)$, no general prediction exists for the mutual diffusion coefficient $D(\phi)$ in a domain of large polymer concentration.[24] Therefore, the measurement of $D(\phi)$ is of special importance. $D(\phi)$ can be determined from integral mass measurements in pressure step experiments. If the mass evolution at short times is dominated by diffusion, $D(\phi)$ can be obtained from the initial slope of the sorption kinetics. For a film deposited onto an impermeable substrate, the mass change $\delta m(t)$ at short time t for small pressure steps is given by[25]

$$\frac{\delta m(t)}{\delta m_\infty} = \frac{2}{\sqrt{\pi}}\sqrt{\frac{Dt}{L^2}} \quad (5)$$

where δm_∞ is the value of δm at equilibrium ($t \to \infty$). For pure Fickian diffusion, a plot of δm versus $t^{1/2}$ results in a straight line for the initial phase of sorption–desorption. For more complicated situations, this linear dependence on $t^{1/2}$ is not observed. However, as long as diffusion dominates at short times [$(\mathrm{DEB})_D > 1$], the slope of $\delta m(t)$

versus $t^{1/2}$ at $t = 0$ can be used to determine the diffusion coefficient D. The main uncertainty originates from the choice of δm_∞ which is influenced by the mechanical relaxation on longer time scales. No true plateau in $\delta m(t)$ develops, and there remains an ambiguity on the value to be chosen for δm_∞.

In the case of a blend, various authors have considered the dependence of χ and T_g on the fraction of the constituents.[22,26] If the 2 polymers are perfectly miscible, these relations are useful for the description of drying. In the Results and Discussion section, we compare our experimental results to the existing models. No prediction exists on the elastic modulus K^0_{gl} nor on the diffusion coefficient D for polymer blends.

MATERIALS AND SAMPLE PREPARATION

We investigated an industrial varnish used by Pechiney Emballage Alimentaire (PEA) for food packaging. It is a blend (30/70) of a vinylic copolymer (V) and an acrylic copolymer (A) (molar masses are about 21,000 and 110,000 g/mol, respectively). The formulation has emerged from practical experience.

The glass transition temperature T_g of the pure copolymers and of the blend was investigated by differential scanning calorimetry (DSC; Fig. 1). The heating rate was 10°C/min. The glass transition temperatures are given in Table I. The glass transition of the acrylic copolymer A is slightly distorted. Possibly, it exhibits some heterogeneities on microscopic scale, which may be related to a nonhomogeneous segment distribution along the copolymer chain. The width is substantially larger for the blend than for the vinylic copolymer but smaller than for the acrylic copolymer. The glass transition temperature of the mixture roughly corresponds to the linear interpolation between the T_g values of the constituents, showing that the 2 constituents are well miscible.[26]

The film surface was investigated by atomic force microscopy (AFM). The 2 copolymers and the blend were studied before and after annealing at 100°C for 14 h. No structure was observed, showing that the 2 copolymers are well miscible on that scale as well.

The following 2 film thicknesses were used: about 1 μm for pressure step experiments, and about 350 nm for quasi-stationary pressure ramps. The 350-nm films were spin cast from a 5% wt solution in methyl ethyl ketone (MEK) (spinning rate $\cong$ 1500 rpm). The 1-μm films were spin-cast from a 10% wt solution in MEK (spinning rate $\cong$ 1700 rpm). Because the vapor pressure of MEK is high, it rapidly evaporates, and obtaining thick and laterally homogeneous samples proved to be problematic. When investigating the surface of the films with a profilometer

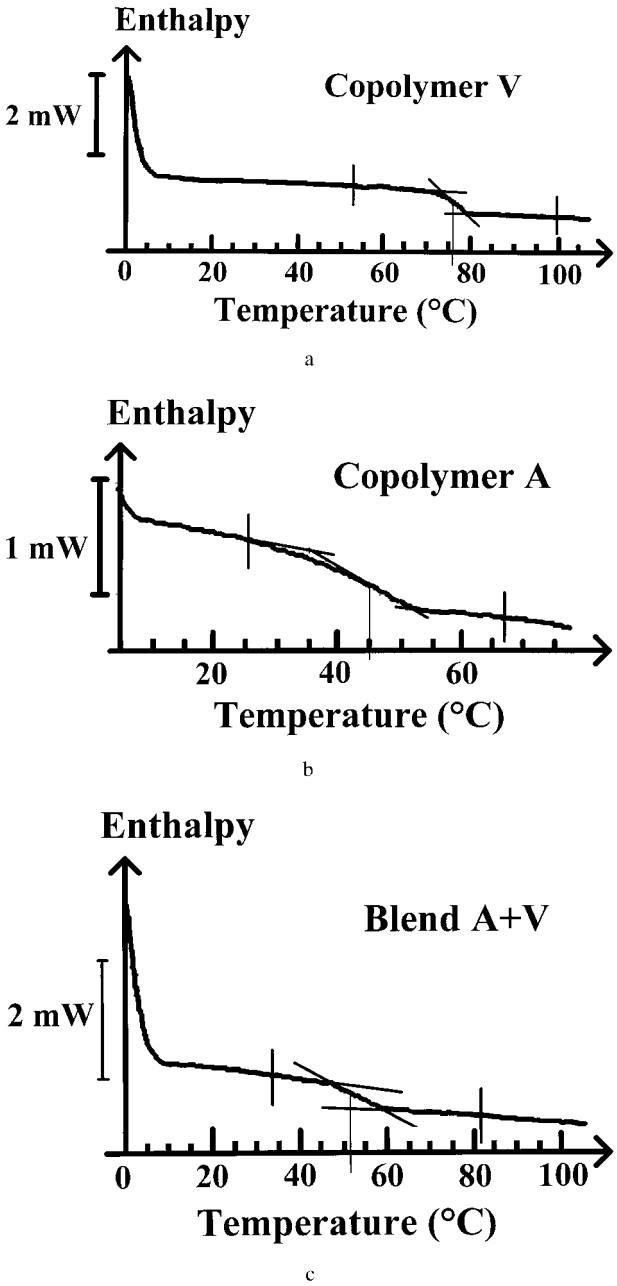

Figure 1 Differential scanning calorimetry data for the vinylic copolymer V (a), the acrylic copolymer A (b), and the A + V blend (c) (70/30 w/w). The glass transition temperature T_g is taken as the midpoint of the transition domain.

Table I Results Obtained Fitting the Pressure Ramps for the Different Systems Under Study: A–MEK, V–MEK, and A + V (70/30)–MEK with the Flory–Huggins [Eq. (3)] and the Leibler–Sekimoto [Eq. (4)] Models

Measurement	A (Pure Acrylic)	A + V Mixture (70/30)	V (Pure Vinylic)
T_g (°C)	45	53	76
χ	0.53 ± 0.05	0.45 ± 0.05	0.28 ± 0.05
ϕ_g	> 0.97	0.95 ± 0.01	0.89 ± 0.01
K^0_{gl} (GPa)	—	0.90 ± 0.25	0.8 ± 0.2
W_g	< 0.02	0.038 ± 0.006	0.07 ± 0.01
a_g	< 0.13	0.20 ± 0.04	0.33 ± 0.03
$(\phi_g)_{\text{Chow}}$	0.975–0.98	0.96	0.87

(Alpha-Step 200 from Tencor Instruments), we found thickness fluctuations in the range of 5–10% of the sample thickness. The lateral scale was tens of microns, that is, much larger than the film thickness. Then we can assume that these variations do not critically affect our results. After spin-coating, we annealed the samples in a vacuum oven for 5 h at 110°C.

MEK (molar mass M_S = 72 g/mol) was chosen as solvent because of its high vapor pressure of 93 Torr at 25.4°C (1 Torr = 1 mmHg = 1.316 mbar).[27] In this way, a large range of vapor pressures is accessible without condensation of liquid on the polymer film. MEK is a good solvent and is also used in the industrial process.

EXPERIMENTAL

Mass Determination

Quartz crystal resonators are a comparatively easy and precise tool to determine the mass of thin films.[28,29] AT-cut, plane parallel quartzes, optically polished, on both sides were used. The fundamental frequency was 4 MHz. The gold electrodes were 150 nm thick. The back electrode had a keyhole shape to achieve energy trapping.[30] The mounting structure was a slightly modified alligator clamp.

When a thin film is coated onto one of the electrodes of a quartz crystal thickness-shear resonator, its acoustical resonance frequencies change due to the weight of the film. For a sufficiently thin film, the relation between mass and frequency change is given by the Sauerbrey equation,[14] as follows:

$$\delta f = -\frac{2 f_f f}{Z_q}\,\delta m \tag{6}$$

where δf is the frequency shift relatively to the unloaded quartz, f is the frequency of a given harmonic, f_f is the frequency of the fundamental, $Z_q = 8.8 \times 10^6$ kg m^{-2} s^{-1} is the acoustic impedance of AT-cut quartz, and δm is the film mass per unit area. Given an accuracy of frequency determination of about 1 Hz, monolayer sensitivity is achieved.

For films whose thickness exceeds one-tenth of the wavelength of transverse (shear) sound, the validity of the Sauerbrey equation is limited: corrections for the viscoelastic behavior of the film have to be applied.[31,32] For polymers below the glass transition (shear modulus $G \cong 10^9$ Pa), this limit is about 10 μm. The wavelength of sound scales as $G^{1/2}$, and the limit can be as low as 1 μm for rubbery materials. When viscoelastic effects are significant, an improved value for the mass per unit area is obtained by plotting the apparent mass $[(Z_q/2f_f)(\delta f/f)]$ measured for different harmonics versus n^2 (n = 1, 3, 5, . . . ; the overtone order) and extrapolating to $n = 0$. The elastic compliance can be estimated from the slope of that same plot. We found that elastic corrections were indeed significant. The shear modulus varies because of the plasticizing effect of the solvent. With the Sauerbrey equation [eq. (6)], one would underestimate the film mass by up to 3% at high solvent content (that is, large elastic compliance).

The data acquisition has been described elsewhere.[31,33] Briefly, we use an HP4195 impedance analyzer (Hewlett–Packard) to determine the frequency-dependent alternating current admit-

tance of the quartz resonator in the vicinity of an acoustic resonance. Because of the piezoelectric effect, the mechanical resonance is seen as a Lorentz curve in the conductance spectrum. Here, and in the following, the conductance $G(\omega)$ and the susceptance $B(\omega)$ are the real and the imaginary part of the admittance $Y(\omega)$, which is the inverse of the impedance $Z(\omega)$. With a nonlinear Levenberg–Marquardt fit algorithm, we determine the center and the bandwidth of the resonance. Data acquisition on one harmonic takes about 10 s. Because the extrapolation procedure to $n = 0$ (n the overtone order) is needed, the frequency measurement has to be repeated on several harmonics (typically $\cong 5$ or 6). Including fitting and extrapolation, mass determination takes about 1.5 min per data point.

For pressure step experiments, this data rate is much too low. A factor of 10 is gained by omitting extrapolation to $n = 0$ and just using the Sauerbrey equation on one given harmonic [eq. (6)]. For still faster measurements, we developed an iterative procedure based on the use of susceptance spectrum $B(\omega)$ instead of conductance spectrum $G(\omega)$. It is assumed that a shift in the resonance frequency only shifts the spectrum without altering it in any other way. First, just before the pressure step, the cursor is placed onto the resonance frequency ω_{ci}, and the slope of the tangent at the susceptance curve, at the frequency ω_{ci}, $p = [dB(\omega)/d\omega]_{\omega=\omega_{ci}}$, is determined. Then, during the pressure step, the resonance frequency $\omega_c(t)$ evolves very quickly, and it is calculated iteratively, as follows (Fig. 2). At time $(t + dt)$, the susceptance is measured at the frequency $\omega = \omega_c(t)$ (which was the resonance frequency at time t), and the resonance frequency at time $(t + dt)$, $\omega_c(t + dt)$ is calculated by a linear interpolation using the slope p. The cursor is then moved to the new frequency $\omega = \omega_c(t + dt)$, and the procedure is iterated. As no frequency sweep occurs, the time resolution is decreased down to $\Delta t \cong 0.2$ s. On the other hand, the accuracy of this procedure must be carefully checked under the different experimental conditions and the height of the pressure step in particular.

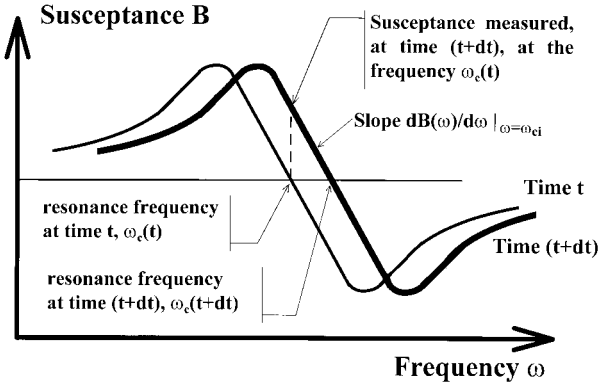

Figure 2 Principle of the fast acquisition algorithm for mass measurement.

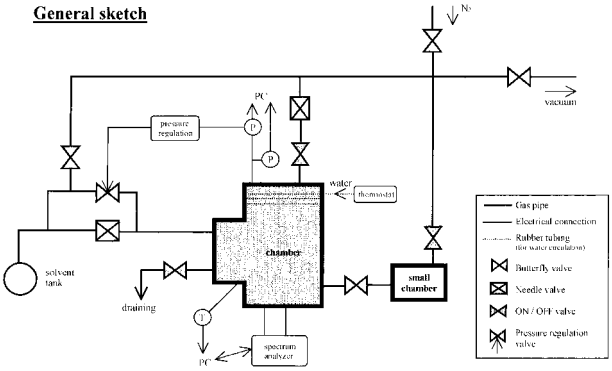

Figure 3 Schematic of the experimental setup. The 2 quartzes in the main vacuum chamber are connected to the impedance spectrum analyzer.

For reasons outlined in a forthcoming publication,[34] it is advantageous to use high harmonics for the extrapolation procedure to $n = 0$. At these high harmonics, the oscillation is confined to the central area of the quartz. For the pressure ramp experiments, we used harmonics 6–12 (44–92 MHz). For pressure step experiments, we measured the frequency shift on the third harmonic because damping was critical, and damping is usually lower on low harmonics.

The temperature inside the chamber was adjusted with a thermostat to $T = 25.4 \pm 0.1$°C. Temperature control is important because temperature couples to the resonance frequency. We found that the temperature fluctuations of $\Delta T \cong 0.1$°C result in an error in mass determination smaller than $\pm 5 \times 10^{-8}$ kg/m^2. This corresponds to an uncertainty in solvent content of $\delta W \cong 2 \times 10^{-4}$ for a 350-nm film (W is the solvent mass reported to the polymer mass).

Setup and Methodology for Sorption–Desorption Experiments

Figure 3 schematically displays the experimental setup. A vacuum chamber was used to adjust the solvent vapor pressure above the polymer film. In equilibrium, the chemical potential μ is the same on both sides of the film–vapor interface. The

chemical potential in the vapor is given by $\mu = kT \ln(a)$, where $a = P/P_{sat}$ is the activity, P is the vapor pressure, and P_{sat} is the saturation vapor pressure of pure solvent. For MEK, we have $P_{sat} = 93$ Torr at 25.4°C.[27] The lowest pressure reached under continuous pumping is 10^{-3} Torr. Since the experiments were undertaken at much larger pressures, we call this state "zero pressure" in the following. Two pressure gauges were used for the ranges $P > 10$ Torr and $P < 10$ Torr. The accuracy was $\delta P \cong 0.1$ Torr for $P > 10$ Torr and $\delta P \cong 10^{-3}$ Torr for $P \leq 10$ Torr.

All samples were annealed in a vacuum oven prior to the experiments. After mounting the sample in the vacuum chamber, we pumped for at least 1 h. The mass of the dry film is then measured. Subsequently, the pump is disconnected, and solvent vapor is introduced from a solvent reservoir outside the chamber. The reservoir is at room temperature. The maximum solvent vapor pressure in the chamber was $P \cong 0.7 \times P_{sat}$.

Two types of experiments were performed, as follows.

1. Quasi-stationary experiments were carried out with slow ramps of decreasing pressure; after equilibrating the film for 45 min at 60 Torr, the vapor is slowly removed through a needle valve. The typical duration of a ramp is 12 h.
2. Pressure step experiments were performed by adding a second small chamber to the setup. This chamber was first evacuated and then closed. Opening a connection between the 2 chambers results in a sudden pressure drop in the main chamber. Typically, $|\Delta P|/P$ is about 0.07, and the time constant is less than 0.2 s.

When working with empty quartzes, we observed that pressure affects the resonance frequency as well. The effect has been described in the literature[28] and has the following 3 sources: viscous drag of the gas, pressure dependence of the elastic constants of the quartz, and desorption of physisorbed molecules from the quartz surface. In some cases, we worked with a reference quartz mounted next to the quartz under investigation. However, we found that the effect was reproducible for quartzes from a given batch. We estimate the systematic error due to pressure effects to be about 4×10^{-8} kg m^{-2} Torr^{-1}. The systematic error in solvent content δW due to pressure is maximal at 65 Torr. For a film thickness around 350 nm, the error δW is less than 1%.

For pressure step experiments, the Sauerbrey relation [eq. (6)] was applied, ignoring all viscoelastic effects. This necessarily increases the error on the solvent content. Quantitatively, for a 5-Torr MEK pressure step and a 350-nm film, we find $\delta(\Delta W) \cong 1\%$ at 65 Torr, and $\delta(\Delta W) \cong 0.1\%$ at $P < 10$ Torr. ΔW represents the whole variation of the solvent content during the step. At 65 Torr, the main contribution to the error comes from the neglect of viscoelastic effects; whereas at low pressures, the pressure effect dominates.

Apart from the systematic errors, we observed a slow and constant drift of the dry mass measured at zero pressure, which is about 0.03% per h. This drift is still not fully understood. Presumably, solvent molecules are trapped inside the film. For the quasi-stationary experiments, the solvent content was calculated with the film mass after complete drying as the state of reference.

In order to estimate the diffusion coefficient $D(\phi)$ for various solvent contents, kinetic experiments were performed; starting from equilibrium (or quasi-equilibrium; that is, the pressure was kept constant for about 10 to 30 min), the pressure was decreased by small successive steps. The amplitude of each step is less than 3 Torr around $P \cong 45$ Torr and less than 0.3 Torr around $P \cong 5$ Torr. Since the pressure increments are small, the diffusion coefficient can be assumed to remain approximately constant during a step. For the polymers and for the solvent contents under study, the maximum value of D is close to 10^{-12} m^2/s. For 1-μm films, the corresponding diffusion time is about 1 s. With a data acquisition speed of 0.2 s (see the Mass Determination section), this is at our experimental limit. Small pressure increments were also essential to ensure that the slope of the susceptance $[dB(\omega)/d\omega]_{\omega=\omega_c}$ remains constant during the step. In fact, a slight change of slope introduces a non-negligible error in the determination of the diffusion constant. Numerical simulation of the error bar shows a relative error of $\delta D/D \cong 1.5$. Since the diffusion coefficient $D(\phi)$ varies over some orders of magnitude, this error bar is acceptable.

The choice of film thickness constitutes the following compromise: for pressure ramp experiments, quasi-stationary diffusion equilibrium is needed. This can only be reached with sufficiently thin films. On the other hand, the measurement of the solvent mass fraction becomes less accurate

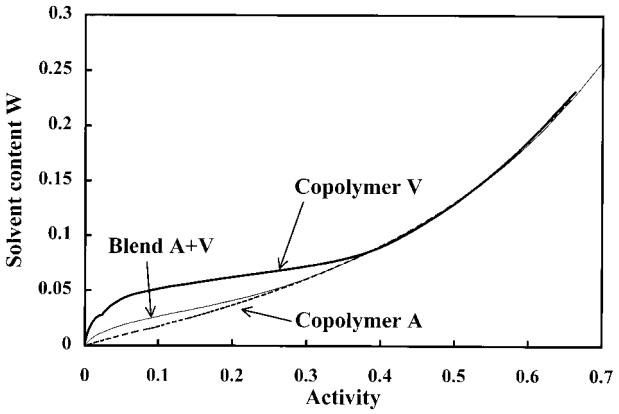

Figure 4 Quasi-stationary desorption data for vinylic and acrylic copolymers and for the A + V blend (70/30 w/w). W is the ratio of solvent mass and polymer dry mass; $a = P/P_{sat}$ is the solvent vapor activity. The pressure ramp has a mean velocity of around 65 Torr in 12 h.

as the total mass (that is, the film thickness) decreases. For pressure step experiments, we have to use thicker films in order to slow down the drying kinetics. Otherwise the mass acquisition algorithm cannot follow. Films thicker than about 1 μm, on the other hand, excessively dampen the resonance when they become soft, which has to be avoided.

RESULTS AND DISCUSSION

Quasi-Stationary Sorption Data

Figure 4 displays the quasi-equilibrium desorption curves for the 3 systems under investigation: pure vinylic (V) and pure acrylic (A) copolymers and the blend A + V. The solvent weight fraction W is defined as $W = (m - m_0)/m_0$, where m is the film mass, and m_0 is the dry mass obtained after a pressure ramp at $P = 10^{-3}$ Torr. We have displayed the solvent content W versus activity a rather than the chemical potential μ versus polymer volume fraction ϕ because this plot is closer to the experiments. The solvent chemical potential is $\mu = kT \ln(a) = kT \ln(P/P_{sat})$, and the polymer volume fraction is $\phi = V_P/(V_P + V_S W)$, where V_P and V_S are the specific volumes of polymer and solvent (expressed in cm^3/g: $V_{MEK} = 1.24$; $V_A = 0.93$; $V_V = 0.74$; $V_{A+V} = 0.87$).

The behavior observed for the 3 materials is quite different. For the vinylic copolymer V, T_g is far above room temperature, and the desorption curve exhibits the kink characteristic of glass transition; for activities higher than about 0.35, the solution is rubbery, and the curve follows the Flory–Huggins model [eq. (3)]. For smaller activities, the solvent content in the film is found to be higher than predicted by the Flory–Huggins law. Finally, W rapidly decreases for activities smaller than 0.05. For the acrylic copolymer A, the glass transition occurs at very low activity so that the kink is hardly discernible at all. As expected, the mixture A + V exhibits an intermediate behavior.

For quantitative analysis, we used the approach by Leibler and Sekimoto[1] (see the Theoretical Background section). The 3 parameters χ, ϕ_g, and K^0_{gl} were determined in 2 steps. First, the interaction parameter χ was derived by fitting the Flory–Huggins law [eq. (3)] to the data in the rubber domain $a > a_m$, where the lower limit a_m is chosen *a priori* from visual inspection of the data. In practice, the determination of χ was found not to be very sensitive on the choice of a_m. In a second step, the 2 parameters ϕ_g and K^0_{gl} were determined by fitting the data in the glass domain $0 \leq a \leq a_m$ with the expression calculated by Leibler and Sekimoto [eq. (4)]. We checked *a posteriori* that the activity a_g corresponding to the glass transition [that is, calculated from eq. (3) knowing ϕ_g; note that for $\phi = \phi_g$, eqs. (3) and (4) lead to the same value for μ, that is, for a] is close to a_m.

Table I summarizes the results of fitting. The experimental data and the fits are compared in Figure 5. In the rubber domain, modeling with a Flory–Huggins law leads to a satisfactory agreement, with slight disagreements in the high pressure range. A better fit can be obtained by introducing an interaction parameter χ varying with the solvent volume fraction.[35,36] These results are not reported here since the solvent content interval available for the fit is too small (less than 0.2) to allow reliably their determination. The focus of this work is the glass transition rather than the χ-parameter, so we do not attempt to enlarge the range of solvent content investigated. The main source of error on the χ-parameters is temperature calibration since the pure solvent-saturating vapor pressure P_{sat} used to calculate the activity strongly depends on temperature. In the glass domain ($a < a_g$), the model introduced by Leibler and Sekimoto describes the experimental data well.

It is interesting to compare the polymer volume fraction at the glass transition ϕ_g for the 2 pure constituents with Chow's prediction,[23] as follows:

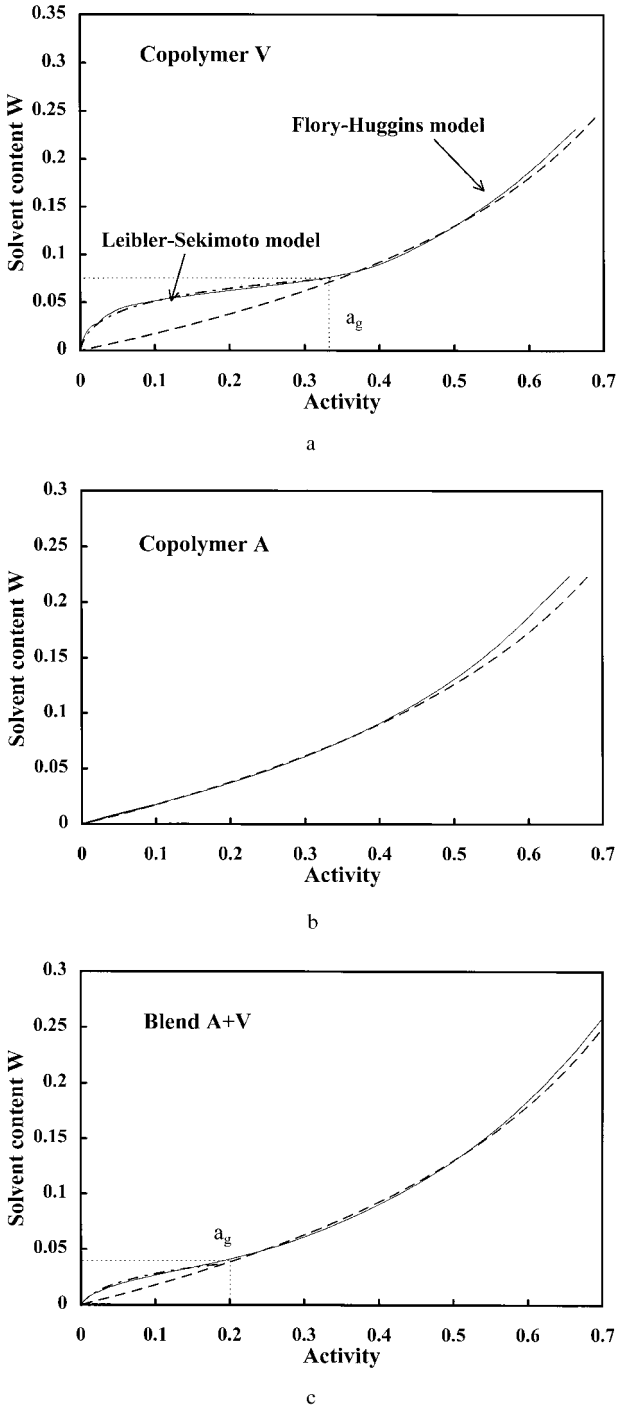

Figure 5 (a–c) Comparison of the experimental desorption data (solid lines) with the Flory–Huggins and the Leibler-Sekimoto models (dashed lines).

$$\ln\left(\frac{T_g}{T_{g0}}\right) = \beta[(1-\theta)\ln(1-\theta) + \theta\ln(\theta)] \quad (7)$$

where T_{g0} is the glass transition temperature of the pure polymer, and T_g the glass transition temperature for the solution having a polymer volume fraction ϕ. The dimensionless parameters β and θ are $\theta = \nu_M(1-\phi)/z\nu_S\phi$ and $\beta = zR/M_M\Delta C_{PP}$, where ν_M and ν_S are the monomer and solvent molecular volumes, respectively, M_M is the monomer molecular weight, z is the lattice coordination number (taken as 2), R is the gas constant, and ΔC_{PP} is the excess isobaric specific heat of transition for the polymer. With the values T_{g0} and ΔC_{PP} estimated from the DSC measurement (see the Materials and Sample Preparation section), eq. (7) leads to the values $\phi_g = 0.87$, 0.98, and 0.96 for the vinylic copolymer V, the acrylic copolymer A, and the blend A + V, respectively. This compares well to the values given in Table I.

In the rubber state, the values found for χ can be used to determine the interaction parameter between acrylic and vinylic copolymers and thus to check their miscibility. From the thermodynamics of ternary solutions, we can set[26]

$$\chi_{A+V} = \frac{\chi_v + r\chi_A}{1+r} - \chi'\frac{r}{(1+r)^2} \quad (8)$$

where χ_{A+V}, χ_A, and χ_V are the Flory–Huggins interaction parameters for the blend and the acrylic and the vinylic copolymers in MEK, χ' is the interaction parameter between the acrylic and vinylic copolymers, and $r = \phi_A/\phi_V$ is the ratio of volume fractions. Inserting numbers, we find $\chi' \cong 8.5 \times 10^{-2}$. This low value confirms the miscibility of the two polymers as found by DSC and AFM investigations.

The assumption that the elastic contribution in the bulk osmotic modulus K^0_{gl} is constant (see the Theoretical Background section) leads to a good description of our data. The order of magnitude of K^0_{gl} is the same for the vinylic copolymer and for the blend. It is also very near to the value found for poly(vinyl chloride)–vinyl chloride mixture, as follows: $K^0_{gl} \cong 1.1$ GPa.[1] The fitted value for K^0_{gl} is an average value from the domain $\phi_g \leq \phi \leq 1$. K^0_{gl} may depend on the polymer matrix structure and, hence, on the history of the film. In particular, changing the pressure ramp velocity (provided diffusion equilibrium is maintained) would allow to investigate the dependence of K^0_{gl} on the drying kinetics.

Pressure Step Experiments

An example of the time evolution of mass and pressure during a pressure step is shown in Fig-

ure 6. Two regimes can be distinguished, as follows. Initially, diffusion dominates and leads to a fast decrease of solvent content. Subsequently, viscoelastic relaxation dominates and results in a rather slow additional drying. We observed a significant viscoelastic effect even at activities above the glass transition. Since the glass transition temperature of the solution at this activity is not very different from the experimental temperature, the departure from a purely Fickian kinetics is not unexpected.

This kinetic looks like the pseudo-Fickian behavior described by several authors for small sorption steps.[9] However, contrary to sorption experiments, which exhibit a large variety of behaviors (case II, 2-step, . . .), a similar kinetic behavior was observed in all our desorption experiments, that is, for all the activities we have studied. Anomalous sorption kinetics is often explained by a wet front between the rubbery and glassy part of the sample.[12] The front moves with a constant velocity presumably related to the polymer matrix disentanglement, and the solvent mass uptake is mainly determined by the front velocity. Our experiments indicate that there is no equivalent front of drying in desorption. Otherwise, we should have observed a desorption kinetics resembling case II or 2-step kinetics.

The determination of the diffusion coefficient was done comparing the experimental points recorded immediately after the pressure step, when diffusion is assumed to be dominant, to the Fick's law predictions. First, since the experimental pressure evolution was sometimes slightly different from a pure Heaviside step, we used a numerical simulation of the mass evolution during the run based on the Fick's law rather than the analytical expression of the initial slope given in eq. (5). This simulation assumed the following boundary conditions: impermeability at the interface substrate–film and concentration condition at the interface film–vapor. The concentration at the outer film surface at each time was deduced from the measured value of P using a linear relationship, the parameters of this relation being evaluated from the values at 2 equilibrium points (before and much later after the pressure step). Secondly, for the pseudo-Fickian behaviors as observed in Figure 6, the determination of D depends on the choice of δm_∞ (see the Theoretical Background section). To overcome this difficulty, we fitted the mass variations for 2 extreme values of δm_∞, as follows: measured well beyond the step end, and the half of this value. The upper and lower limits of error bars reported in Figure 7 correspond to these extreme values.

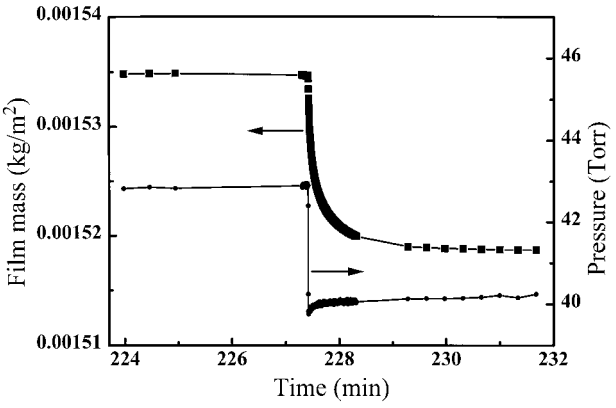

Figure 6 Typical traces of pressure and mass during a pressure step for the vinylic copolymer (film thickness, 1 μm; pressure step, 42.9 to 40.2 Torr corresponding to the activity step, 0.46 to 0.43).

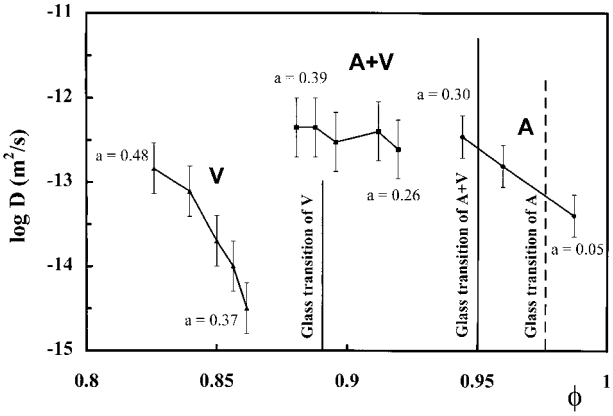

Figure 7 Mutual diffusion coefficient D of MEK in the vinylic copolymer V, the acrylic copolymer A, and in the blend A + V (70/30 w/w) as a function of polymer volume fraction.

The results obtained for the 3 systems with the corresponding activities and polymer contents are displayed in Figure 7. Only a limited range of concentrations could, up to now, be investigated with a good accuracy. In spite of this restriction, the proposed method was found to be suitable for the diffusion coefficient study in the concentrated polymer domain where only very few experimental results are available. A large decrease of D is observed for the vinylic copolymer, as follows: D drops from $10^{-12.7}$ to $10^{-14.5}$ m^2/s between $\phi = 0.82$ and $\phi = 0.86$. The acrylic copolymer also exhibits a significant decrease in the mutual diffusion coefficient between ϕ equal to 0.94 and 0.98.

These variations are characteristic of the hypodiffusive behavior exhibited by such systems in the concentrated domain.[37] Qualitatively, the diffusion coefficients for the blend are intermediate to the values found for the components. A more accurate analysis of the transport behavior of the blend compared to the diffusion characteristics of its components deserves further investigations.

CONCLUSIONS

Quartz microbalances were used to study the drying of polymer solutions in the concentrated domain. The great accuracy of quartz resonators allows the investigation of films less than 1 μm thick. At this low thickness, diffusion equilibrium can be reached in a few minutes even in the glassy domain so that quasi-stationary sorption–desorption experiments become feasible. From these slow desorption experiments, the solvent chemical potential $\mu(\phi)$ as a function of polymer volume fraction ϕ could be derived. The mutual diffusion coefficient $D(\phi)$ could be obtained from pressure step experiments. These variations were investigated in the concentrated domain for which only few results are available in the literature. The influence of the glass transition was analyzed. Since drying was the principal aim of this study, we confined ourselves to desorption experiments.

We studied an industrial varnish, which is a blend of 2 copolymers, as well as the 2 components of the blend separately. The variation of the solvent chemical potential $\mu(\phi)$ with polymer volume fraction was deduced from ramps of slowly decreasing pressure, starting from a highly swollen rubber state and terminating in a dry glassy state. Since the 2 components have different glass transition temperatures, T_{g0}, they behave differently; for the vinylic one, the glass transition occurs for an activity of about $a_g \cong 0.35$, and the plot of solvent content versus activity exhibits the characteristic deviation from the Flory–Huggins law. Since the acrylic copolymer has a T_{g0} near room temperature, the effect is much weaker in this material and, in fact, is hardly observable. The blend shows an intermediate behavior.

For analysis, we used the model proposed by Leibler and Sekimoto,[1] which connects the excess solvent uptake in the glass state to the finite rigidity of the polymer matrix and a concomitant elastic contribution to the osmotic modulus. The fit parameters are the polymer–solvent interaction parameter χ, the polymer volume fraction at the glass transition ϕ_g, and the elastic contribution to the bulk osmotic modulus K^0_{gl}. The agreement between the experimental results and the model is very good. For the 3 systems studied, the polymer volume fraction at the glass transition ϕ_g is in good agreement with Chow's predictions.[23]

The mutual diffusion coefficients were deduced from pressure step experiments. The mass variation shows the 2 following regimes: a first one with fast desorption governed by diffusion, and a second with slow desorption governed by viscoelastic relaxation. We find a decrease of the diffusion coefficient as the polymer concentration increases; this is typical of the hypodiffusive behavior of polymer solutions. Only results obtained in the concentration domain very close to the glass transition have been reported here. A next step will consist in studying the behaviors of the 2 pure constituents and of the blend in the glassy domain.

This work was supported by Pechiney Emballage Alimentaire, France. The authors also thank M. Daoud for helpful discussions.

REFERENCES

1. L. Leibler and K. Sekimoto, *Macromolecules,* **26,** 6937 (1993).
2. P. Neogi, *Diffusion in Polymers,* Dekker, New York, 1996.
3. K. Tanaka, J.-S. Yoon, A. Takahara, and T. Kajiyama, *Macromolecules,* **28,** 934 (1995).
4. J. S. Vrentas, J. L. Duda, H.-C. Ling, and A.-C. Hou, *J. Polym. Sci., Polym. Phys. Ed.,* **23,** 289 (1985).
5. T. S. Frick, W. J. Huang, M. Tirrell, and T. P. Lodge, *J. Polym. Sci., Part B: Polym. Phys.,* **28,** 2629 (1990).
6. R. A. Waggoner and F. D. Blum, *J. Coating Technol.,* **61,** 51 (1989).
7. B. Guerrier, C. Bouchard, C. Allain, and C. Bénard, *AIChE J.,* **44,** 731 (1998).
8. R. A. Cairncross, S. Jeyadev, R. F. Dunham, K. Evans, L. F. Francis, and L. E. Scriven, *J. Appl. Polym. Sci.,* **58,** 1279 (1995).
9. G. F. Billovits and C. J. Durning, *Macromolecules,* **27,** 7630 (1994).
10. A. R. Berens, *Makromol. Chem., Macromol. Symp.,* **29,** 95 (1989).
11. N. L. Thomas and A. H. Windle, *Polymer,* **23,** 529 (1982).
12. G. Rossi, P. A. Pincus, and P.-G. De Gennes, *Europhys. Lett.,* **32,** 391 (1995).

13. J. S. Vrentas and J. L. Duda, *AIChE J.,* **25,** 1 (1979).
14. G. Sauerbrey, *Arch. Elektrotech. Übertragung,* **18,** 617 (1964).
15. M. Sanopoulou, P. P. Roussis, and J. H. Petropoulos, *J. Polym. Sci., Part B: Polym. Phys.,* **33,** 993 (1995).
16. T. P. Gall and E. J. Kramer, *Polymer,* **32,** 265 (1991).
17. P. F. Nealey, R. E. Cohen, and A. S. Argon, *Polymer,* **36,** 3687 (1995).
18. T. P. Gall, R. C. Lasky, and E. J. Kramer, *Polymer,* **31,** 1491 (1990).
19. J. S. Vrentas and C. M. Vrentas, *J. Polym. Sci., Part B: Polym. Phys.,* **32,** 187 (1994).
20. P. J. Flory, *Principles of Polymer Chemistry,* Cornell University Press, New York, 1953.
21. A. R. Berens, *Polymer Eng. Sci.,* **20,** 95 (1980).
22. J. D. Ferry, *Viscoelastic Properties of Polymers,* Wiley, New York, 1980.
23. T. S. Chow, *Macromolecules,* **13,** 362 (1980).
24. R. A. Waggoner, F. D. Blum, and J. M. D. MacElroy, *Macromolecules,* **26,** 6841 (1993).
25. J. Crank, *Mathematics of Diffusion,* Oxford University Press, London, 1956.
26. O. Olabisi, L. M. Robeson, and M. T. Shaw, *Polymer–Polymer Miscibility,* Academic Press, New York, 1979.
27. I. Mellan, *Industrial Solvent Handbook,* Noyes, USA, 1977.
28. C. Lu and A. W. Czanderna, *Applications of Piezoelectric Quartz Crystal Microbalances,* Elsevier, Amsterdam, 1984.
29. C. D. Stockbridge, *Vacuum Microbalance Techniques,* Vol. 5, Plenum, New York, 1966.
30. V. E. Bottom, *Introduction to Quartz Crystal Unit Design,* Van Nostrand Reinhold, New York, 1982.
31. D. Johannsmann, K. Mathauer, G. Wegner, and W. Knoll, *Phys. Rev. B,* **46,** 7808 (1992).
32. A. Domack and D. Johannsmann, *J. Appl. Phys.,* **80,** 2599 (1996).
33. A. Domack, Ph.D. thesis, Universität Mainz, 1996.
34. O. Wolff, E. Seydel, and D. Johannsmann, submitted.
35. J. Brandrup and E. H. Immergut, *Polymer Handbook,* 3rd ed., Wiley-Interscience, 1989.
36. I. Noda, Y. Higo, N. Ueno, and T. Fujimoto, *Macromolecules,* **17,** 1055 (1984).
37. D.-H. Hwang and C. Cohen, *Macromolecules,* **17,** 1679 (1984).